On wakes and near-wall behavior in coarse large-eddy simulation of channel flow with wall models and second-order finite-difference methods

By W. Cabot, J. Jiménez[1] AND J. S. Baggett[2]

1. Motivation & goals

Many high Reynolds number, wall-bounded turbulent flow applications are still too expensive to compute with well resolved large-eddy simulation (LES), which requires resolutions nearly as fine as direct numerical simulation (DNS) near walls. Baggett *et al.* (1997) estimated that well resolved LES of channel flow would require a number of grid points scaling as Re_τ^2, where Re_τ is the friction Reynolds number, based on the requirement that the mesh capture most of the energy-containing scales, which become very small approaching the walls. Thus high Reynolds number flows, especially in complex geometries, become exorbitantly expensive to compute. Approximate wall boundary conditions are needed to avoid computing the fine-scale, near-wall regions and to allow the LES mesh to be determined solely by large outer flow scales and geometry.

In many engineering applications involving turbulence in complex geometries, low-order numerical differencing schemes are often employed because they are easy to implement and, for central differencing schemes, have good conservation properties. The subgrid-scale (SGS) model and the wall model must also be fairly simple to implement and computationally inexpensive if they are to gain widespread acceptance. It is therefore of practical interest to examine the performance of fairly simple wall models applied to the standard second-order central finite difference codes employed in many codes at CTR, despite the fact that the numerical errors seriously degrade the effective resolution of the simulation and the accuracy of the SGS model (Lund & Kaltenbach 1995, Ghosal 1996, Kravchenko & Moin 1997).

When wall stress models are used in conjunction with very coarsely meshed LES of channel flow, the near-wall points in the outer LES flow are observed to be poorly predicted (e.g., Nicoud *et al.* 1999, Nicoud & Baggett in this volume), with the mean flow moving too rapidly with respect to the core flow. In the channel this means that the skin friction is overpredicted for a given bulk mass flux. This problem also occurs in the attached boundary layers and can lead to poor predictions of separation in flows experiencing adverse pressure gradients farther downstream. Another anomalous feature of these coarse simulations is the lack of any significant "wake" region in the core of the flow, which is observed in experiments and in well resolved DNS and LES.

1 Also with the School of Aeronautics, Univ. Politécnica Madrid.

2 Currently with the Department of Mathematics, Univ. of Wisconsin at La Crosse

Our goal in this report is to present some LES results of channel flow on very coarse meshes which exhibit these symptoms and to attempt to determine the likely sources of error contributing to them. We will also discuss briefly what needs to be done in future work to fix or work around these problems.

2. Results

2.1 Numerical setup

The LES code used in this study was essentially the same one used by Lund & Kaltenbach (1995), but modified to use wall stresses from model routines instead of computing viscous stresses directly from the wall gradients, which are not resolved on the extremely coarse meshes that we use. The code uses a second-order central finite-difference scheme on a staggered mesh and a third-order Runge-Kutta time advancement scheme. A fractional step method is used that updates the pressure at each substep in the Runge-Kutta time advancement (keeping the flow field divergence-free at all times) and keeps the solution for the velocity field strictly second-order in time. The standard dynamic SGS model (Germano *et al.* 1991, Lilly 1992) is implemented with test filtering and averaging on horizontal planes.

The numerical domain for the channel simulations are $2\pi \times 2 \times 2\pi/3$ in units of channel half-width δ in the streamwise (x), wall-normal (y), and spanwise (z) directions, respectively, with periodic boundary conditions in the horizontal (x, z) directions. We note that these dimensions are probably marginally too small to resolve the largest scales properly in a periodic domain. Uniform meshes were chosen with 32^3 and 64^3 computational cells. This gives a very coarse resolution near the walls that is incapable of resolving the energy-bearing scales there. However, because the grid is uniform in all directions, there are no numerical errors due to grid stretching. Target friction Reynolds numbers $Re_\tau = u_\tau \delta/\nu = 650$, 1030, 4000, and 20000 were computed, where ν is the coefficient of molecular viscosity and u_τ is the friction speed. A constant mean streamwise force f was applied, and in steady state the mean streamwise wall stress $\tau_w = u_\tau^2 = f\delta$, which is supplied from wall stress model.

In the second-order scheme, the viscous wall stress for the horizontal velocity components is normally computed from a one-sided difference of the velocity at first off-wall point using the no-slip value at the wall. This expression is replaced in the code with the wall stress from the wall model so that the wall values of horizontal velocities are not actually specified, and one can consider them to be slip velocities. A problem does arise in computing the SGS eddy viscosities in the center of the computational cells along walls, where values of strain and stress tensors are required and which, like wall values, cannot be determined on the coarse grid. Some of the usual recourses are to use the usual expressions with no-slip values at the walls or to use one-sided differences and averages from the interior; we have used the latter for the results shown here. As it turns out, though, the velocity field is so unphysical near the walls that it is probably not possible to get an accurate determination of the SGS stresses there based on the outer flow in any case.

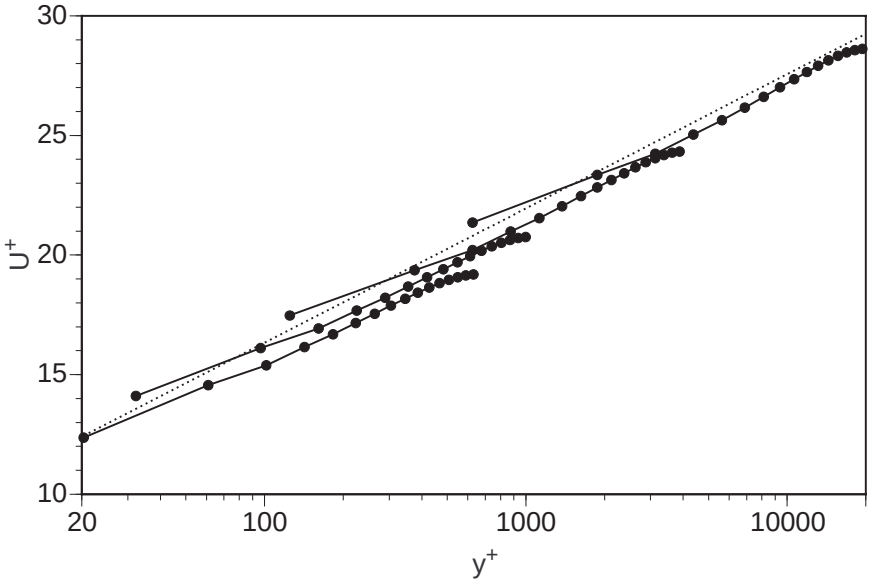

FIGURE 1. Mean streamwise velocity in wall units for LES with TBLE wall stress models on a 32^3 mesh at nominal $Re_\tau = 650$, 1030, 4000, 20000 (—●—). For comparison a log law (Eq. 1) using $\kappa = 0.41$ and $B = 5.1$ is shown (·····).

2.2 Wall stress models

Wall stresses were predicted (1) by matching the interior horizontal speed to an instantaneous log law,

$$U_m = u_\tau \left[\kappa^{-1} \ln(y_m u_\tau / \nu) + B \right] \ , \tag{1}$$

where U_m is the horizontal speed in the outer flow at a distance y_m from the wall (usually in the first or second off-wall computational cells), $\kappa \approx 0.4$ is von Kármán's constant (inverse log law slope), and $B \approx 5$ is the log law interceptor; or (2) by solving the thin boundary layer equations (TBLE) on a fine near-wall grid (Cabot 1995). A comparison of results between these two models, and the results using Piomelli *et al.*'s (1989) shifted model (Nicoud *et al.* 1999, Nicoud & Baggett in this volume), confirmed the earlier finding of Cabot (1995) that there are no significant differences in results between these wall models when applied to channel flow.

2.3 Near-wall behavior

Mean streamwise velocities U are shown in Fig. 1 which all exhibit the same shape with anomalously high values in the first two or three grid points near the wall. Because the outer flow is matched at these high values, the core flow is too low. In Fig. 2 we find that the streamwise rms velocity fluctuations u' are much too high near the wall compared with Kravchenko *et al.*'s (1996) well resolved LES. This is observed mostly in the first 4 or 5 points in the vicinity of the wall. This behavior is also a well known symptom of LES with poor horizontal resolution in the near-wall region, even though very fine wall-normal meshes may be employed.

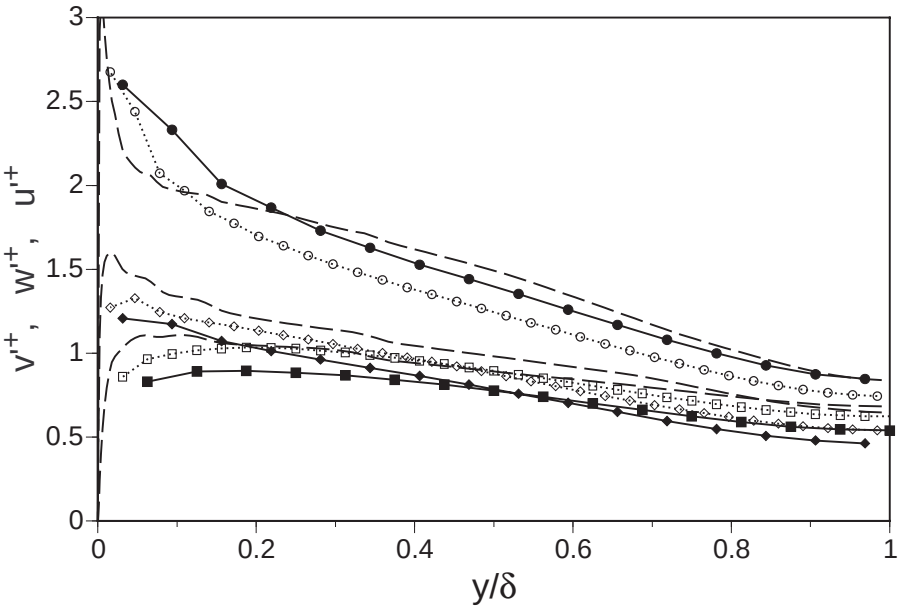

FIGURE 2. Velocity fluctuation intensities for LES with TBLE wall stress models at $Re_\tau = 4000$ on a 32^3 mesh (——— , closed symbols) and on a finer 64^3 mesh (····· , open symbols). For comparison the well resolved zonal LES data of Kravchenko *et al.* (1996) at $Re_\tau = 4000$ is shown (— — —).

Another useful way of viewing the anomalous near-wall behavior of U is that the wall-normal gradients of U are too small in the near-wall region, since this is the way in which it enters the mean momentum balance:

$$\tau_w \approx (\nu + \nu_s) dU/dy + R_{12} + fy \,, \tag{2}$$

where ν_s is the mean SGS eddy viscosity and $R_{12} = -\overline{u'v'}$ is the resolved Reynolds shear stress. One might suspect that the eddy viscosity is too high near the wall, but an examination of its behavior in Fig. 3 shows the opposite to be true: the dynamic Smagorinsky coefficient and the eddy viscosity actually tend to drop dramatically in the grid points nearest the wall. Porté-Agel *et al.* (1999) have recently shown that this occurs as a function of the grid spacing rather the physical spacing (and which we have confirmed in comparing the 32^3 with the 64^3 mesh results); they suggest that this behavior results from applying the dynamic procedure inappropriately to large, energy-bearing scales that do not act self-similarly.

An arbitrary means of enhancing the near-wall SGS eddy viscosity was employed in which C was fit linearly to its interior values from the 4th off-wall point to about 0.5δ. This is partially justified by consideration that the flow at the first off-wall stations is already well in the log layer and should not experience strong wall blocking effects. This causes C to be nearly constant (as in the original Smagorinsky model) and ν_s to increase rapidly near the wall as seen in Fig. 3. The effect of this in Eq. (2) is to provide a large amount of dissipation near the wall that reduces R_{12} much more that it increases the term $\nu_s dU/dy$. Since the other terms in Eq. (2) are

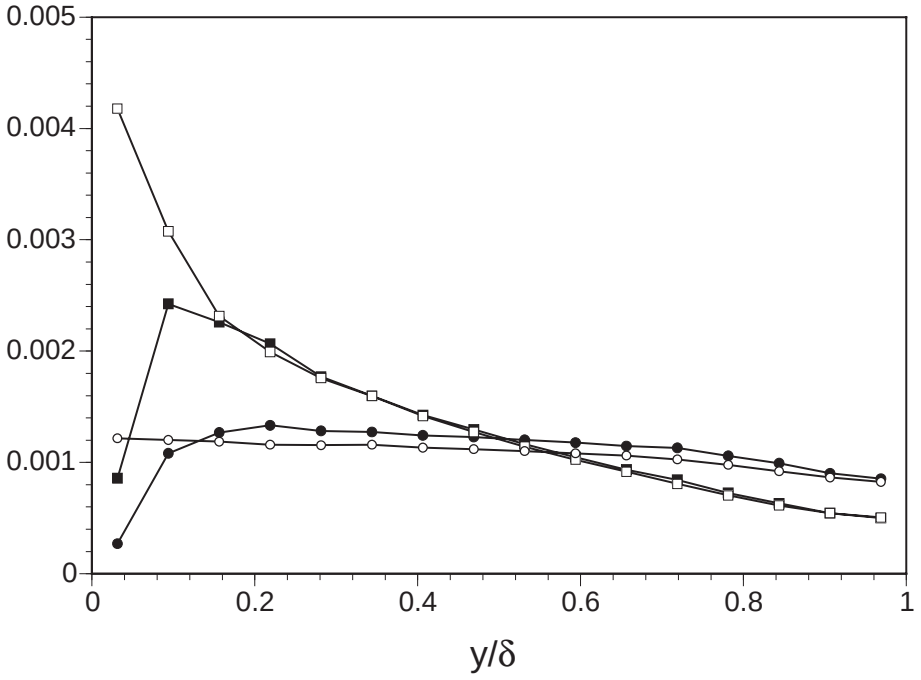

FIGURE 3. The mean SGS eddy viscosity ν_s in units of $u_\tau\delta$ (■) and coefficient $20C\Delta^2/\delta^2$ (●) for the dynamic Smagorinsky model (Germano *et al.* 1991) for LES on a 32^3 mesh at $Re_\tau = 4000$. Curves with open symbols were specially modified near the wall while curves with closed symbols were unmodified.

fixed in steady state, the response of the flow is to steepen the slope of U near the wall. This has the effect of straightening out the profile U toward the logarithmic profile as shown in Fig. 4. While the rms streamwise velocity u' is seen to drop at the first off-wall point in Fig. 5, the anisotropy in velocity fluctuations is seen to get even worse farther out in the flow. Baggett (1998) speculated that boosting the eddy viscosity (either by this method or by shifting to a RANS description) merely causes the near-wall flow to behave like one at a much lower Reynolds number, which may explain the shift outward in the peak of u'. The effects of this enhancement are of course much less pronounced on the finer 64^3 grid as seen in Fig. 6 for mean velocity profiles, although it still improves the results noticeably.

It should be noted that the mean streamwise velocity profile near the wall is also found to be more log-like when a stretched grid is used or when there are other large numerical errors that act in a dissipative manner. This was observed by Cabot (1995) using a first-order accurate time advancement scheme with large time steps. On the face of it, it may seem that more model dissipation is called for near the poorly resolved wall where the model would be expected to carry much more of the stresses and dissipation. But there is also the fact that the velocity field on such coarse meshes is unphysical and has fluctuations that are preternaturally large. Baggett (1998) has suggested that enormous pseudo-streaks form on the scale of the grid (which is much larger than the physical spacing of natural streaks of about

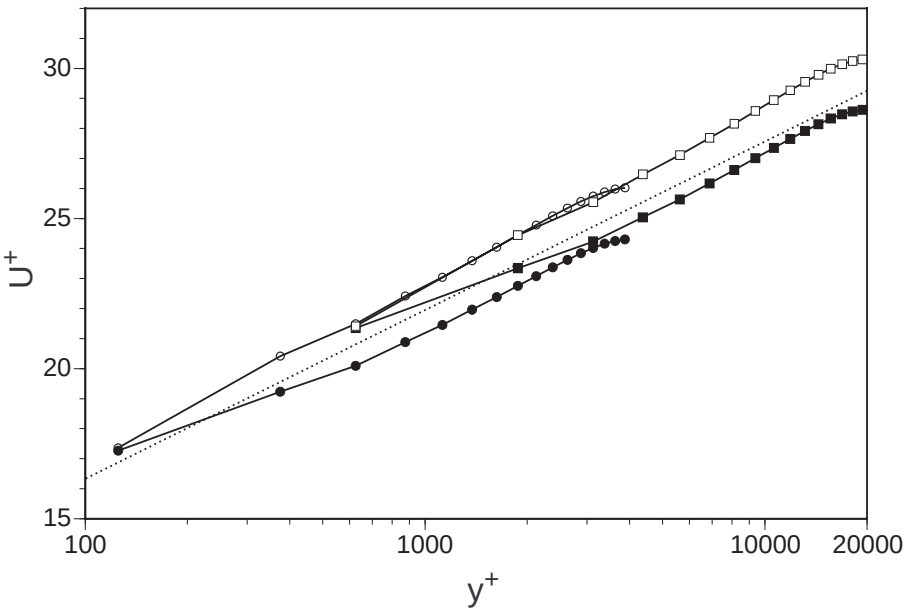

FIGURE 4. Mean streamwise velocity in wall units for LES with TBLE wall stress models on a 32^3 mesh at nominal $Re_\tau = 4000$ and 20000 with (open symbols) and without (closed symbols) enhanced SGS eddy viscosity near the walls. For comparison a log law (Eq. 1) using $\kappa = 0.41$ and $B = 5.1$ is shown (·····).

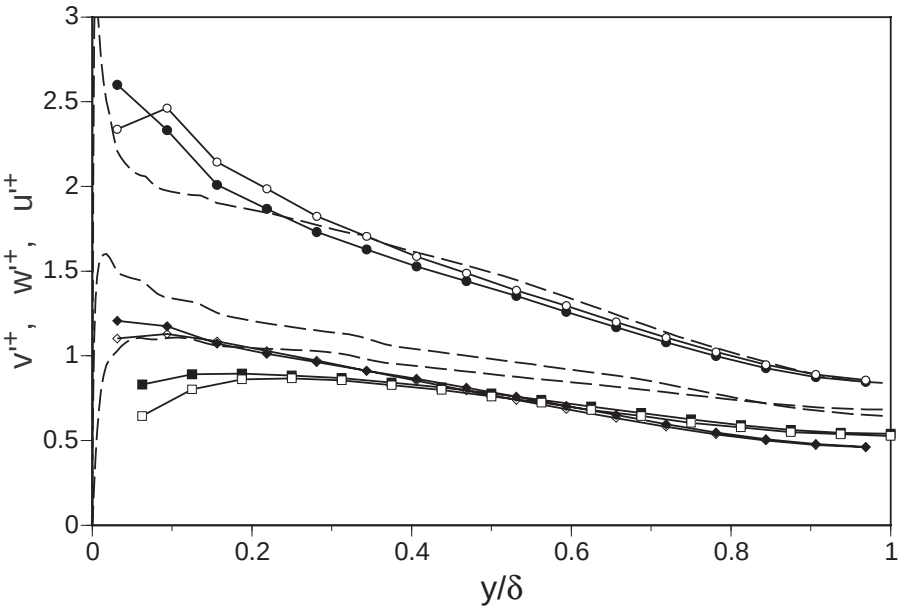

FIGURE 5. Velocity fluctuation intensities for LES with TBLE wall stress models on a 32^3 mesh at $Re_\tau = 4000$ with (open symbols) and without (closed symbols) enhanced SGS eddy viscosity near the walls. For comparison the well resolved LES data of Kravchenko *et al.* (1996) at $Re_\tau = 4000$ is shown (———).

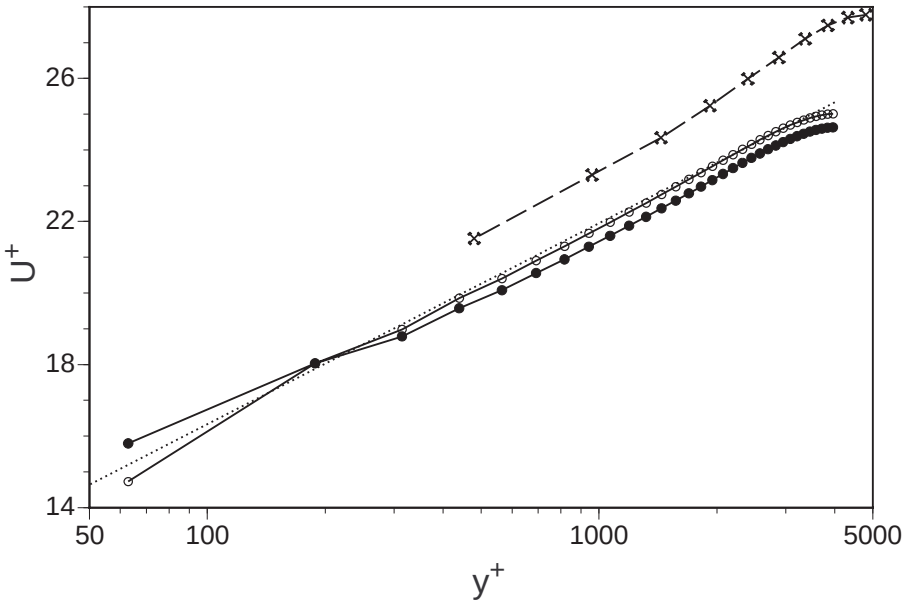

FIGURE 6. Mean streamwise velocity in wall units for LES with an instantaneous log law wall stress model on a finer 64^3 mesh at $Re_\tau = 4000$ with (open symbols) and without (closed symbols) enhanced SGS eddy viscosity near the walls. For comparison a log law (Eq. 1) using $\kappa = 0.41$ and $B = 5.1$ is shown (·····). Experimental data by Comte-Bellot (1965) for $Re_\tau = 4800$ (– – × – –) shows the typical shape of the wake.

100 wall units) and that velocities in these unnatural structures have excessively large fluctuation values. Indeed the reason SGS models using stochastic backscatter (Mason & Thomson 1992) obtain better mean velocity profiles may be that they prevent these structures from forming. Good mean profiles were also obtained using wall stresses derived from a suboptimal matching of a target log law (Nicoud *et al.* 1999, Nicoud & Baggett in this volume); these wall stresses have large fluctuations that may also act to disrupt the formation of unphysical streak-like structures.

We also note that the dynamic mixed model (Zang *et al.* 1993), though often touted as superior to the standard dynamic model in some situations, does quite a bit worse in this case. A run with this model produced large near-wall stresses with little accompanying dissipation from the similarity term, and it reduced the dissipation from the Smagorinsky term. This acts in exactly the wrong way in Eq. (2), boosting the resolved stress even higher than before and causing dU/dy to decrease even further near the wall.

The issue of how to generate good near-wall velocity profiles is, therefore, still rather unsettled from the modeling standpoint. It may in fact be too much to ask that we can ever get the nearest two or so points near the wall to behave physically. The numerical error in second-order finite-difference methods is such that the effective resolution is no better than one in three points compared with a spectral method. Applying this logic to the near-wall region suggests that something like the first two or three points away from the wall are doomed to be unreliable

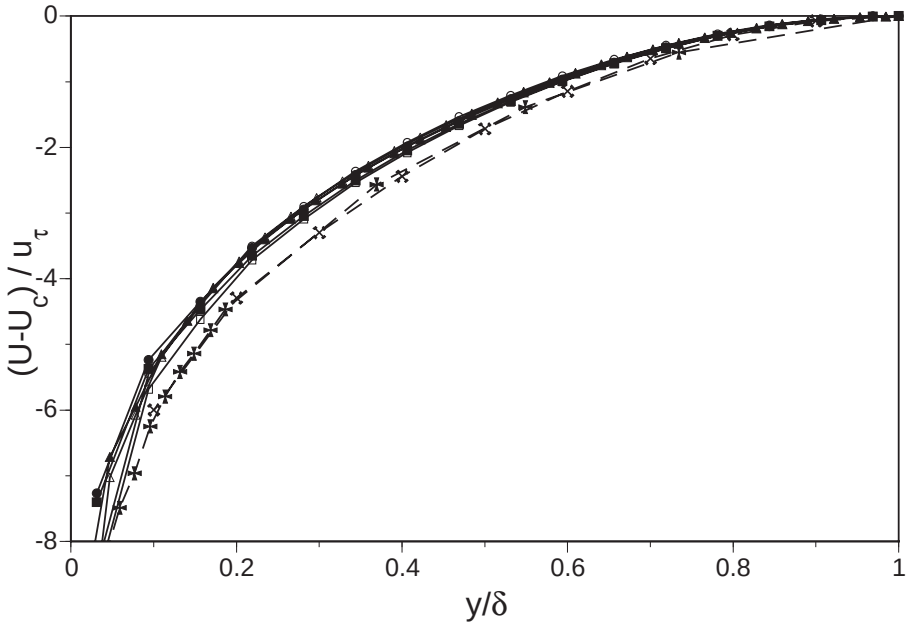

FIGURE 7. Defect plot for LES with wall stress models on a coarse 32^3 mesh and finer 64^3 mesh at $Re_\tau = 4000$ and 20000 (———) with (open symbols) and without (closed symbols) enhanced SGS eddy viscosity near the walls. For comparison, experimental data (- - - -) for $Re_\tau = 1655$ (+ , Wei & Willmarth 1989) and 4800 (× , Comte-Bellot 1965) are shown.

simply because of the poor numerical resolution caused by the finite-differencing scheme. It should be possible to determine the expected behavior of stresses and strains, and the eddy viscosity derived therefrom, measured in *a priori* tests of coarsely filtered DNS and LES with well resolved walls. However, converting this information into a successful RANS-like model for the near-wall region may be much more difficult in practice (Baggett 1998).

2.4 Wake behavior

A notable feature of the mean streamwise velocity profiles for the very coarse 32^3 meshed in Fig. 1 is the lack of any significant wake-like feature in the core of the flow. Even streamwise velocity profiles on finer 64^3 mesh (Fig. 6), show no noticeable wake compared with experimental data or well resolved simulations. A more direct way of viewing the core flow is to plot the mean velocity profile in outer units as a defect $(U - U_c)/u_\tau$ with respect to the centerline velocity U_c, which is shown in Fig. 7 for several of the coarse LES runs with wall models and for some experimental data. The LES defects are seen to be much too shallow compared with the experimental values, again indicative of a much smaller wake.

Standard fits of the log-wake region (e.g., Dean 1976) give a defect law that depends only on the slope of the log law (κ^{-1}), the wake parameter Π, and the position in outer units (y/δ):

$$(U - U_c)/u_\tau = \kappa^{-1}[\ln(y/\delta) - 2\Pi + G(y/\delta)] \,, \tag{3}$$

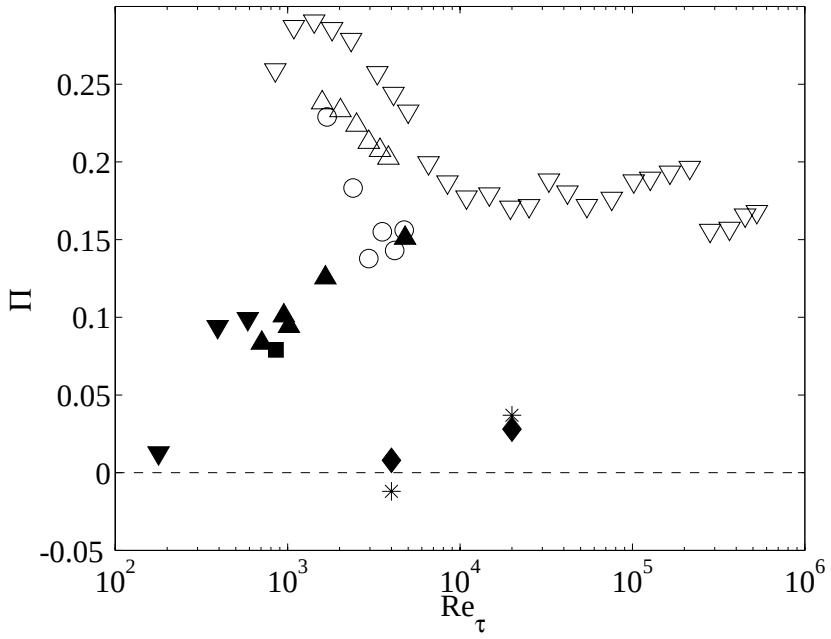

FIGURE 8. Wake parameter as a function of friction Reynolds number for AGARD (1998) channel and pipe flow data: DNS channel data (▾) (Kim *et al.* 1987, Moser *et al.* 1999), experimental channel data (▴) (Wei & Willmarth 1989, Comte-Bellot 1965), and experimental pipe flow with smooth walls (▵ , Perry *et al.* 1986; ▿ , Zagarola & Smits 1997) and with rough walls (∘ , Perry *et al.* 1986). Results from a well resolved LES at $Re_\tau = 1000$ (▪ , Kravchenko *et al.* 1996) and from the LES with wall models presented here at $Re_\tau = 4000$ and 20000 with (∗) and without (⬥) enhanced SGS viscosity near the walls.

where $G(x) \equiv (1 + 6\Pi)x^2 - (1 + 4\Pi)x^3$. Typical values of Π are roughly 0.1 for channels and 0.2 for pipes. In Fig. 8 we have plotted a number of values of Π from channel and pipe experiments and simulations. The wake parameters for our very coarse LES are virtually zero, similar in fact to the classic low Reynolds number DNS case by Kim *et al.* (1987) at $Re_\tau = 180$. It would appear then that the cumulative sum of all our modeling and numerical errors results in an essentially low Reynolds number flow. We note too that enhancing the near-wall SGS eddy viscosity, which represents a sizable change in the boundary condition, has almost no effect on the results, already indicating that the near-wall conditions are probably not to blame here. Nicoud *et al.* (1999, also see Nicoud & Baggett in this volume) used a rather violent wall stress boundary condition, but their very coarse simulations also exhibit the same (lack of) wake behavior as ours.

We also note that the rough pipe data (Perry *et al.* 1986) shows somewhat smaller wakes than their smooth counterparts. It is tempting to speculate that this difference in boundary condition causes differences in the core flow, but the difference between smooth and rough wake parameters is fairly minor compared with the

difference between coarse LES and resolved simulations, and no other major differences in core turbulence intensity or length scales between smooth and rough walls is found in Perry's data to suggest that this is in fact the case.

The real culprit appears instead simply to be poor resolution, as found previously in the resolution tests by Lund & Kaltenbach (1995) for this second-order code in a $Re_\tau = 2000$ channel. Their coarsest simulations had a stretched wall-normal grid that resolved the viscous region and about the same streamwise resolution and twice the spanwise resolution as our finer (64^3) mesh cases; mean velocity profiles from these simulations also showed virtually no wake. However, when they increased their horizontal resolution by a factor of 3/2, a small wake became evident. And when they increased the initial horizontal resolution by a factor of 3, a large wake was found — larger in fact than the typical experimental wake. This is due to the fact that they were using a numerical domain of $\pi\delta/2$ in the span, which is known to be much too small to resolve large core structures in a periodic domain. Even "well resolved" LES by Kravchenko *et al.* (1996) using a domain of $\pi\delta/2$ in the span gave a huge, unphysical wake, while results at $Re_\tau = 1000$ with a $\pi\delta$ spanwise domain gave good agreement with experimental wake parameters as shown in Fig. 8.

The effects of poor resolution in the second-order code are amplified using the standard dynamic procedure for the SGS model. The second-order differencing causes roughly the lower two-thirds of the velocity spectrum to be corrupted. The standard dynamic procedure then uses this corrupted information to predict an inaccurate Smagorinsky coefficient and SGS stresses. Only when the grid is padded by a factor of 3 or more and explicit filtering is used to removed the erroneous high-wavenumber information, or if a grid is used that is large enough such that the residual SGS stresses are negligible anyway, will one obtain accurate results in the core flow irrespective of the wall model.

3. Future work

It became evident in the course of this work that much better and more extensive experimental data exists for turbulent pipe flow, smooth and rough (see Fig. 8), and it would be very useful to perform coarse LES for pipes using wall models and finite-difference methods. It would also be interesting to explore further the possible correspondence between wall roughness and wall models to clarify the effects that wall boundary conditions have on the interior flow.

Simulations of channel flow with wall models using higher fidelity numerics (e.g., spectral-spline methods) should be attempted to remove some of the numerical resolution issues encountered in this work and allow a clearer assessment of the wall model performance.

It may be unavoidable having the flow in the first few grid points in the vicinity of the wall be corrupted by inadequate resolution in low-order finite difference codes. In that event, the flow calculation there serves no useful purpose other than acting as an artificial buffer region. In particular, flow data at these near-wall grid points should not be used for matching to the log law or any other near-wall RANS model to determine wall stresses. More accurate flow conditions from beyond the

contaminated region should be used instead, and any details about the steady-state inner flow should be constructed from a detailed RANS solution. In boundary layers with separation, the situation becomes somewhat more difficult because details about the growth of the boundary layer and separation depend to a large degree on the near-wall momentum, which may be grossly inaccurate using wall stress models and low-order numerical schemes. In this case, and perhaps in some time developing cases, it may be possible to develop an iterative scheme in which a detailed inner RANS solution is computed occasionally and used to readjust the wall stress model for the outer flow solution. Simulations with large separation regions such as turbulent flow behind a step and around a cylinder may provide good test cases for this kind of scheme.

This work is supported by the AFOSR.

REFERENCES

AGARD 1998 A selection of test cases for the validation of large-eddy simulations of turbulent flows. *Advisory Report 345*, NATO, chap. 5, 109-128.

Baggett, J. S., Jiménez, J., & Kravchenko, A. G. 1997 Resolution requirements in large-eddy simulations of shear flows. *Annual Research Briefs 1997*, Center for Turbulence Research, NASA/Stanford Univ., 51-66.

Baggett, J. S. 1998 On the feasibility of merging LES with RANS for the near-wall region of attached turbulent flows. *Annual Research Briefs 1998*, Center for Turbulence Research, NASA/Stanford Univ., 267-277.

Cabot, W. 1995 Large-eddy simulations with wall models. *Annual Research Briefs 1995*, Center for Turbulence Research, NASA/Stanford Univ., 41-50.

Comte-Bellot, G. 1965 Ecoulement turbulent entre deux parois paralleles. *Publ. Sci. et Tech. du Ministere de l'Air no. 419.*

Dean, R. B. 1976 A single formula for the complete velocity profile in a turbulent boundary layer. *ASME J. Fluids Eng.* **98,** 723-727.

Germano, M., Piomelli, U., Moin, P., & Cabot, W. H. 1991 A dynamic subgrid-scale eddy viscosity model. *Phys. Fluids A* **3**, 1760-1765. Erratum: *Phys. Fluids A* **3**, 3128.

Ghosal, S. 1996 An analysis of numerical errors in large-eddy simulations of turbulence. *J. Comp. Phys.* **125,** 187-206.

Kim, J., Moin, P. and Moser, R. D. 1987 Turbulence statistics in fully developed channel flow at low Reynolds number. *J. Fluid Mech.* **177,** 133-166.

Kravchenko, A. G. and Moin, P. 1997 On the effects of numerical errors in large-eddy simulations of turbulent flows. *J. Comp. Phys.* **131,** 310-322.

Kravchenko, A. G., Moin, P. and Moser, R. D. 1996 Zonal embedded grids for numerical simulations of wall-bounded turbulent flows. *J. Comp. Phys.* **127,** 412-423.

Lilly, D. 1992 A proposed modification of the Germano subgrid-scale closure method. *Phys. Fluids A* **4**, 633-635.

Lund, T. S. and Kaltenbach, H.-J. 1995 Experiments with explicit filtering for LES using a finite-difference method. *Annual Research Briefs 1995*, Center for Turbulence Research, NASA/Stanford Univ., 91-105.

Mason, P. J. and Thomson, D. J. 1992 Stochastic backscatter in large-eddy simulations of boundary layers. *J. Fluid Mech.* **242,** 51-78.

Moser, R. D., Mansour, N. N. and Kim, J. 1999 Direct numerical simulation of turbulent channel flow up to $Re_\tau = 590$. *Phys. Fluids* **11**, 943-945.

Nicoud, F., Baggett, J., Moin, P. and Cabot, W. 1999 LES wall-modeling based on optimal control theory. Submitted to *Phys. Fluids*.

Perry, A. E., Henbest, S. M. and Chong, M. S. 1986 A theoretical and experimental study of wall turbulence. *J. Fluid Mech.* **165,** 163-199.

Piomelli, U., Ferziger, J., Moin, P. and Kim, J. 1989 New approximate boundary conditions for large eddy simulations of wall-bounded flows. *Phys. Fluids* **1**, 1061-1068.

Porté-Agel, F., Meneveau, C. and Parlange, M. B. 1999 A scale-dependent dynamic model for large-eddy simulation: application to a neutral atmospheric boundary. Submitted to *J. Fluid Mech.*

Wei, Y. and Willmarth, W. W. 1989 Reynolds-number effects on the structure of a turbulent channel flow. *J. Fluid Mech.* **204,** 57-95.

Zagarola, M. V. and Smits, A. J. 1997 Scaling of the mean velocity profile for turbulent pipe flow. *Phys. Rev. Lett.* **78,** 239-242.

Zang., Y., Street, R. L., & Koseff, J. R. 1993 A dynamic mixed subgrid-scale model and its application to turbulent recirculating flows. *Phys. Fluids A* **5**, 3186-3196.